Available online at www.sciencedirect.com
SCIENCE DIRECT
Optics Communications 261 (2006) 13–18
OPTICS COMMUNICATIONS
www.elsevier.com/locate/optcom

Total internal reflection diffraction grating in conical mounting

L. Eisen *, M.A. Golub, A.A. Friesem

Department of Physics of Complex Systems, Weizmann Institute of Science, P.O. Box 26, Rehovot 76100, Israel

Received 17 August 2005; received in revised form 16 November 2005; accepted 28 November 2005

Abstract

The main conditions and parameters for obtaining surface relief total internal reflection diffraction gratings in conical mounting are presented. Calculated and experimental investigations reveal that there are ranges of grating periods, incidence angles, diffraction angles and gratings depths for which such gratings could be obtained, both for TE and TM polarizations. With optimized grating parameters the diffraction efficiency of the total internal reflection diffraction gratings can be greater than 90%.

PACS: 42.40.Lx; 42.25.Fx; 42.40.Eq; 42.79.Dj

Keywords: Diffraction grating; Holographic grating; Total internal reflection

1. Introduction

During the last three decade surface relief diffraction gratings became an integral part of many modern optical systems and devices including imaging systems [1,2], array illuminators [3], pulse shapers [4], and beam splitters and deflectors [5,6]. Some of the investigations were extended to include surface relief diffraction gratings that also involve total internal reflection (TIR) in the substrate on which the gratings are recorded. These included theoretical investigations of surface relief dielectric gratings in classical (Littrow) mounting [7] as well as subsequent experimental investigations [8]. In such classical mounting, the grating vector and all diffraction orders lie in the plane of incidence.

In this paper, we investigate surface relief TIR diffraction gratings in conical mounting, where the plane of incidence does not contain the grating vector, and determine the relevant conditions and parameters for such gratings. These are then used to design and experimentally record surface relief TIR diffraction gratings in conical mounting that have high diffraction efficiency and where the diffraction angle into the first order is equal to that of the incidence angle, so the diffracted light continues to propagate by TIR. Such gratings in conical mounting can be exploited in planar optics configurations [9,10].

2. Basic conditions for TIR diffraction gratings in conical mounting

A typical three-dimensional conical diffraction geometry for TIR diffraction gratings is schematically presented in Fig. 1. The surface relief TIR diffraction grating is recorded on a transparent substrate of refractive index n_{sub} that is surrounded with a material (typically air) of refractive index n_{sup}, where $n_{\text{sub}} > n_{\text{sup}}$. A linearly polarized monochromatic light beam, propagating inside the substrate, is obliquely incident onto the TIR diffraction grating at the polar angle θ_{inc} and azimuthal angle ϕ_{inc}. The TE polarization is perpendicular to the plane of incidence and the TM polarization lies in the plane of incidence.

The well known grating equations for the diffraction gratings in conical mounting [11] can be written as

* Corresponding author. Tel.: +972 8 9344433; fax: +972 8 9344109.
E-mail address: leon.eisen@weizmann.ac.il (L. Eisen).

0030-4018/$ - see front matter
doi:10.1016/j.optcom.2005.11.064

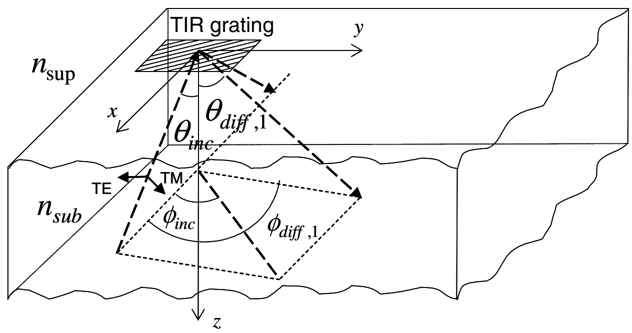

Fig. 1. Typical conical diffraction geometry for the TIR diffraction gratings.

$$\frac{2\pi}{\lambda} n_{\mathrm{sub}} \sin(\theta_{\mathrm{diff},m}) \cos(\phi_{\mathrm{diff},m}) = -\frac{2\pi}{\lambda} n_{\mathrm{sub}} \sin(\theta_{\mathrm{inc}}) + \frac{2\pi}{\Lambda} m \cos(\phi_{\mathrm{inc}}), \tag{1}$$

$$\frac{2\pi}{\lambda} n_{\mathrm{sub}} \sin(\theta_{\mathrm{diff},m}) \sin(\phi_{\mathrm{diff},m}) = \frac{2\pi}{\Lambda} m \sin(\phi_{\mathrm{inc}}), \tag{2}$$

where λ is the wavelength of the incident light, Λ the grating period, $\theta_{\mathrm{diff},m}$ the polar diffraction angle of m diffraction order, and $\phi_{\mathrm{diff},m}$ the azimuthal diffraction angle of the m diffraction orders. The condition for TIR is that no transmitted diffraction orders exist while reflected orders do [7], so that

$$\frac{n_{\mathrm{sup}}}{n_{\mathrm{sub}}} \leqslant |\sin(\theta_{\mathrm{inc}})| \leqslant 1. \tag{3}$$

Using Eqs. (1) and (2) together with Eq. (3), we determined that at certain wavelength, incidence angles and refractive indices, there will be an upper and lower bounds for the range of grating periods beyond which the TIR condition will not hold. Specifically, the maximum and minimum allowable periods Λ_{max} and Λ_{min} are

$$\Lambda_{\mathrm{max}} = \frac{\lambda}{n_{\mathrm{sub}} \sin(\theta_{\mathrm{inc}}) \left[\cos(\phi_{\mathrm{inc}}) + \sqrt{\frac{n_{\mathrm{sup}}^2}{n_{\mathrm{sub}}^2 \sin^2(\theta_{\mathrm{inc}})} - \sin^2(\phi_{\mathrm{inc}})}\right]} \tag{4}$$

and

$$\Lambda_{\mathrm{min}} = \frac{\lambda}{n_{\mathrm{sub}} \sin(\theta_{\mathrm{inc}}) \left[\cos(\phi_{\mathrm{inc}}) + \sqrt{\frac{1}{\sin^2(\theta_{\mathrm{inc}})} - \sin^2(\phi_{\mathrm{inc}})}\right]}. \tag{5}$$

In this range of grating periods only the 0 and 1st reflected diffraction orders exist (i.e. $m = 0,1$). Note that in classical mounting, where $\phi_{\mathrm{inc}} = 0$, Eqs. (4) and (5) readily reduce to the usual simple relation of $\Lambda_{\mathrm{max,L}}$ and $\Lambda_{\mathrm{min,L}}$ for Littrow mounting [12], as

$$\Lambda_{\mathrm{max,L}} = \frac{\lambda}{2n_{\mathrm{sup}}}, \quad \Lambda_{\mathrm{min,L}} = \frac{\lambda}{2n_{\mathrm{sub}}}. \tag{6}$$

3. Design and optimization procedures

Using Eqs. (4) and (5), we calculated the minimum and maximum TIR diffraction grating periods Λ_{min} and Λ_{max} as a function of the polar incidence angle θ_{inc} for three selected azimuthal incidence angles ϕ_{inc}. For these calculations we assumed a sinusoidal surface relief diffraction grating formed on a glass substrate with refractive index $n_{\mathrm{sub}} = 1.52$, free-space wavelength of incident light as $\lambda = 0.6328$ μm, and the selected three azimuthal incidence angles were $\phi_{\mathrm{inc}} = 30°$, 45°, 60°. The calculated results are presented in Fig. 2 as the boundaries of the allowable range of TIR diffraction grating periods. As shown, the range of TIR diffraction grating periods differs at each polar incidence angle θ_{inc} and each azimuthal incidence angle ϕ_{inc}. This range broadens and the minimum period Λ_{min} is larger as the incidence angle ϕ_{inc} increases.

We now consider a specific example of TIR diffraction grating in conical mounting where the polar diffraction angle $\theta_{\mathrm{diff,1}}$ equals that of the incidence angle θ_{inc}, and the azimuthal diffraction angle differs from that of the incidence angle. With $\theta_{\mathrm{inc}} = \theta_{\mathrm{diff,1}}$, Eqs. (1) and (2) lead to an expression for the TIR grating period $\Lambda(\theta_{\mathrm{inc}} = \theta_{\mathrm{diff,1}})$, as

$$\Lambda(\theta_{\mathrm{inc}} = \theta_{\mathrm{diff,1}}) = \frac{\lambda \cos(\phi_{\mathrm{inc}})}{n_{\mathrm{sub}} \sin(\theta_{\mathrm{inc}})(1 + \cos(\phi_{\mathrm{diff,1}}))} = \frac{\lambda \sin(\phi_{\mathrm{inc}})}{n_{\mathrm{sub}} \sin(\theta_{\mathrm{inc}}) \sin(\phi_{\mathrm{diff,1}})}. \tag{7}$$

According to Eq. (7) the azimuthal diffraction angle is the twice that of the incident angle

$$\phi_{\mathrm{diff,1}} = 2\phi_{\mathrm{inc}}. \tag{8}$$

Alternatively, Eq. (7) could be readily obtained from direct observation of the TIR diffraction grating geometry of Fig. 1. The calculated results for $\Lambda(\theta_{\mathrm{inc}} = \theta_{\mathrm{diff,1}})$ as a function of θ_{inc} are shown by the solid curve in Fig. 2. As evident this period decreases to Λ_{min} at the higher incidence angles θ_{inc} for all three azimuthal diffraction angles.

Using rigorous coupled wave analysis algorithms [13], we initially numerically calculated first order diffraction efficiency for a TIR diffraction grating with $\Lambda(\theta_{\mathrm{inc}} = \theta_{\mathrm{diff,1}})$ as a function of grating depth d for a number of selected incidence angles and $\phi_{\mathrm{diff,1}} = 120°$. The results for TE and TM polarizations are presented in Fig. 3. As evident, the diffraction efficiency has alternating maxima and minima, with the highest occurring at grating depths that range from 1 μm to 2 μm for TE polarization. For example, with an incidence angle of and a grating period of $\Lambda(\theta_{\mathrm{inc}} = \theta_{\mathrm{diff,1}}) = 0.6224$ μm, the diffraction efficiency is about 0.9831 for a grating depth of $d = 1.3900$ μm with a corresponding aspect ratio of $\Lambda/d = 2.23$. For TM polarization, high diffraction efficiencies occur at grating depths ranging between 0.2 and 0.5 μm, indicating a significantly lower aspect ratio which is more practical than with TE polarization.

We then calculated the optimal TIR diffraction grating depth d that will provide the maximum first order diffrac-

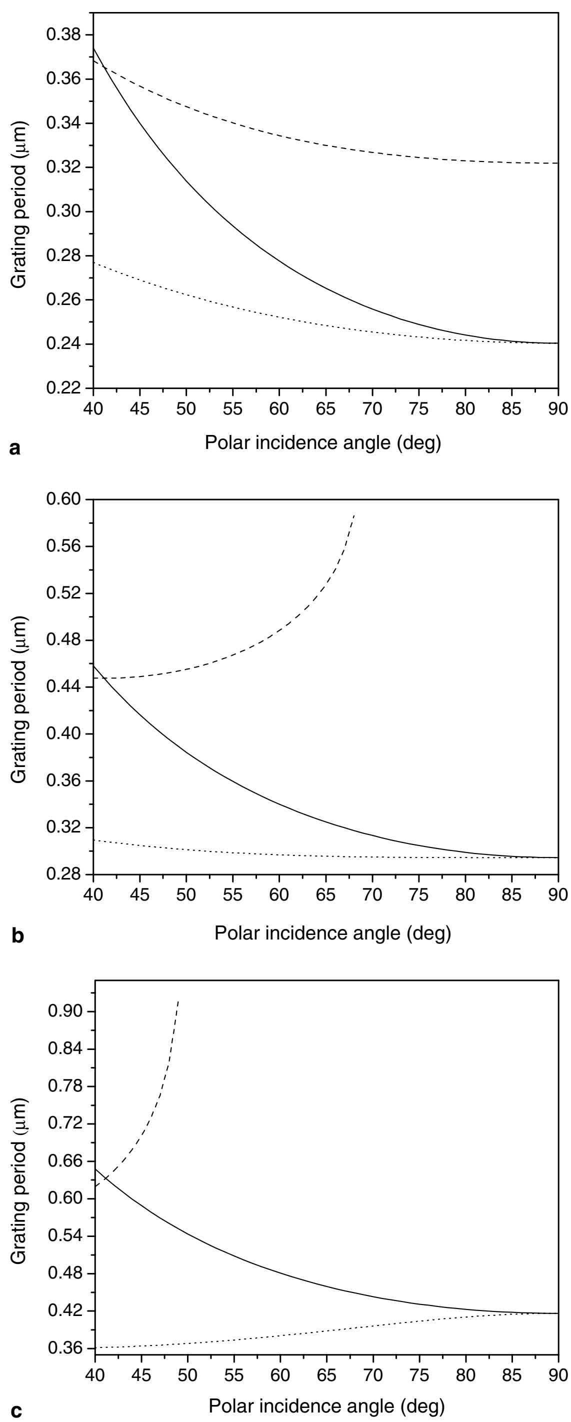

Fig. 2. Boundaries of allowable range of TIR grating periods (dashed curves) and TIR grating period $\Lambda(\theta_{\rm inc}=\theta_{\rm diff,1})$ (solid curve) as a function of incidence angles $\theta_{\rm inc}$ for three different azimuthal diffraction angles: (a) $\phi_{\rm diff,1}=60°$; (b) $\phi_{\rm diff,1}=90°$; (c) $\phi_{\rm diff,1}=120°$.

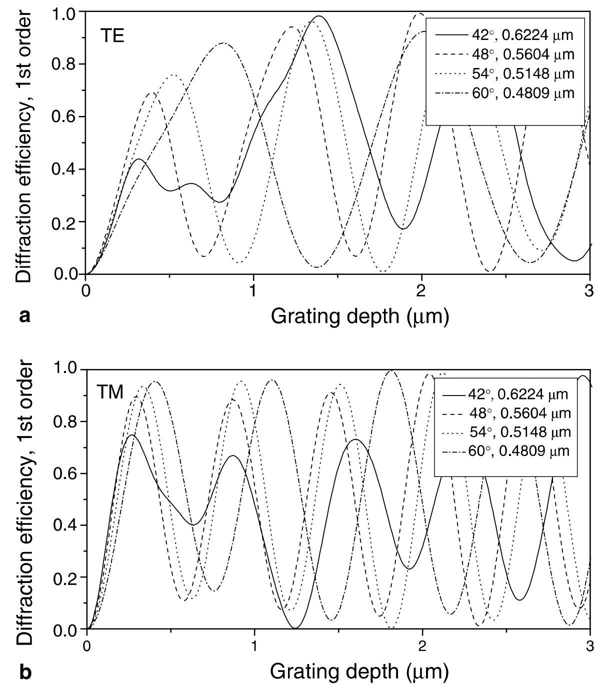

Fig. 3. First order diffraction efficiencies for the TIR gratings with four different periods $\Lambda(\theta_{\rm inc}=\theta_{\rm diff,1})$ and four different incidence angles $\theta_{\rm inc}$ as a function of grating depth d for $\phi_{\rm diff,1}=120°$ and TE and TM light polarizations: (a) TE polarization; (b) TM polarization.

tion efficiency as a function of incidence angle $\theta_{\rm inc}$, both for TE and TM polarizations and for three different azimuthal diffraction angles $\phi_{\rm diff,1}$. The results are presented in Fig. 4. These reveal that high diffraction efficiencies are possible over a wide range of the incident angles $\theta_{\rm inc}$, and that a much smaller aspect ratio is needed for TM polarization. It is interesting to note that for a polar incidence angle $\theta_{\rm inc}=45°$ and a corresponding grating period $\Lambda(\theta_{\rm inc}=\theta_{\rm diff,1})=0.3400$ μm, the diffraction efficiency is about the same for both TE and TM polarizations, at a fixed optimized grating depth of $d=0.4200$ μm. The procedure for optimizing the grating depth for sinusoidal profiles can be extended for optimizing the depth of gratings with more general surface profiles.

Finally, we considered the spectral dispersion of a TIR diffraction grating in conical mounting. We started with the grating dispersion relation for the first diffraction order, which was derived from Eq. (1), as

$$\frac{d\theta_{\rm diff,1}}{d\lambda}=\left|\frac{\cos(\phi_{\rm inc})}{\Lambda\cos(\theta_{\rm diff,1})\cos(\phi_{\rm diff,1})}\right| =\left|\frac{\cos(\phi_{\rm inc})}{\Lambda\cos(\theta_{\rm diff,1})(1-2\sin^2(\phi_{\rm inc}))}\right|. \qquad (9)$$

Using Eq. (9) we calculated the dispersion for a specific TIR diffraction grating in conical mounting, when the azimuthal diffraction angle is $\phi_{\rm diff,1}=60°$, polar incidence angle $\theta_{\rm inc}=44°$ and period $\Lambda(\theta_{\rm inc}=\theta_{\rm diff,1})=0.3461$ μm. The TIR diffraction grating dispersion was determined as $d\theta_{\rm diff,1}/d\lambda=6.9$ mrad/nm. A deviation of the grating period of $\Delta\Lambda=\pm\,0.0033$ μm results in a deviation of $\Delta\theta_{\rm diff,1}=1°$ for the polar diffraction angle.

4. Experimental procedure and results

To experimentally verify our calculated results, we found it convenient to resort to optical configuration comprised

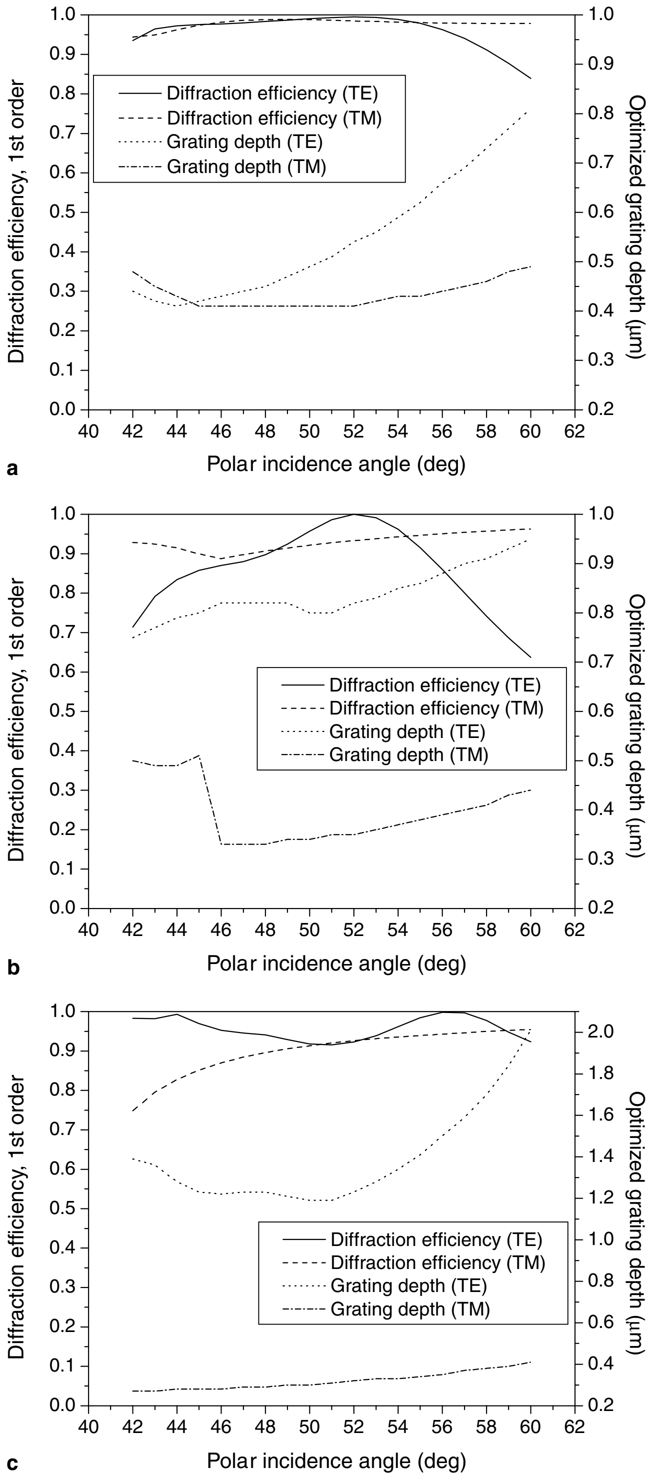

Fig. 4. Optimal grating depth and maximum diffraction efficiency as a function of polar incidence angles θ_{inc} for three different azimuthal diffraction angles $\phi_{diff,1}$: (a) $\phi_{diff,1} = 60°$; (b) $\phi_{diff,1} = 90°$; (c) $\phi_{diff,1} = 120°$. Both TE and TM polarizations are presented.

of two laterally displaced nearly sinusoidal surface relief gratings, arranged as shown schematically in Fig. 5. One merely served to couple an incident light into the substrate and direct it towards the TIR diffraction grating. The gratings were obtained by recording the interference pattern of

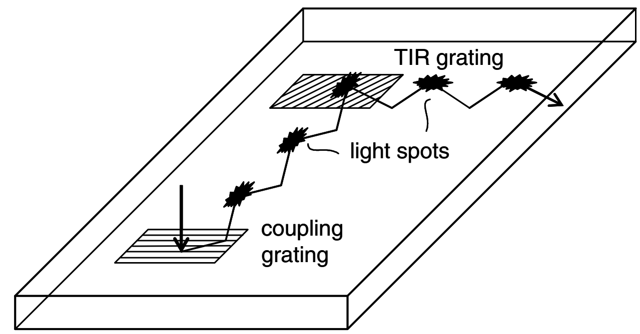

Fig. 5. Arrangement of two diffraction gratings on transparent substrate. Spots correspond to light beam bounces at the substrate surface.

two plane waves, that were derived from an Argon laser of wavelength $\lambda = 0.3630$ µm, in Shipley Ultra-i 123 photoresist layer which was spin coated on a BK-7 glass substrate with refractive index of $n_{sub} = 1.52$.

We recorded three different TIR diffraction gratings, each with a corresponding coupling grating. One TIR diffraction grating had a period of $\Lambda = 0.3461$ µm and depth $d = 0.4100$ µm, while the corresponding coupling grating had a period of $\Lambda = 0.5990$ µm. The coupling grating diffracts a normally incident light beam of $\lambda = 0.6328$ µm into the substrate at an angle of 44°, and the angular orientation between the grating vectors of the two gratings was controlled to be 30°. Accordingly, the polar angular orientation of the beam incident onto the TIR grating will be $\theta_{inc} = 44°$, azimuthal incidence angle $\phi_{inc} = 30°$ and azimuthal diffraction angle $\phi_{diff,1} = 60°$. The second TIR diffraction grating had a period of $\Lambda = 0.4401$ µm and depth $d = 0.5000$ µm, while the corresponding coupling grating had a period of $\Lambda = 0.6220$ µm. The coupling grating diffracts a normally incident light beam into the substrate at an angle of 42°, and the angular orientation between the grating vectors of the two gratings was controlled to be 45°. Accordingly, the polar angular orientation of the beam incident onto the TIR grating will be $\theta_{inc} = 42°$, azimuthal incidence angle $\phi_{inc} = 45°$ and azimuthal diffraction angle $\phi_{diff,1} = 90°$. The third TIR diffraction grating had a period of $\Lambda = 0.4911$ µm and depth $d = 0.3800$ µm, while the corresponding coupling grating had a period of $\Lambda = 0.4910$ µm. The coupling grating diffracts a normally incident light beam into the substrate at an angle of 58°, and the angular orientation between the grating vectors of the two gratings was controlled to be 60°. Accordingly, the polar angular orientation of the beam incident onto the TIR grating will be $\theta_{inc} = 58°$, azimuthal incidence angle $\phi_{inc} = 60°$ and azimuthal diffraction angle $\phi_{diff,1} = 120°$.

The TIR diffraction gratings in conical mounting were then evaluated by illuminating the coupling gratings with incident light beam of wavelength $\lambda = 0.6328$ µm derived from a He–Ne laser. First, we detected the light spots that are scattered from the surface of the substrate which correspond to light bounces inside the substrate, as schematically depicted in Fig. 5. The results are shown in Fig. 6. As

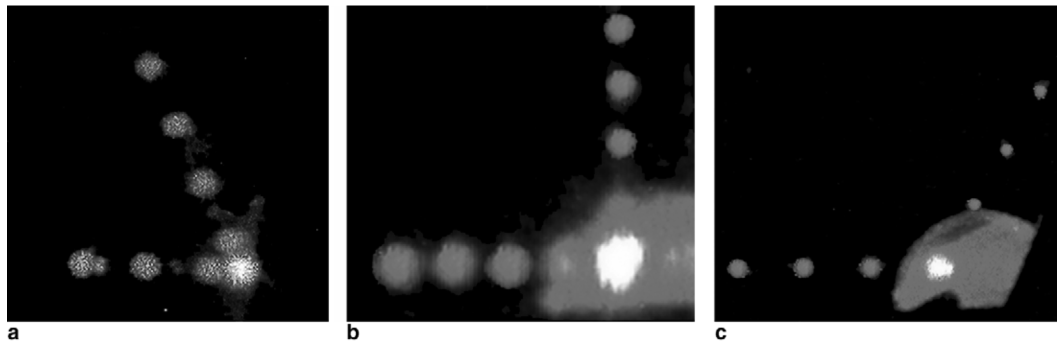

Fig. 6. Experimental detection of light bounces inside a substrate showing angular orientation of diffraction from a TIR grating in conical mounting: (a) $\phi_{\text{diff},1} = 60°$; (b) $\phi_{\text{diff},1} = 90°$; (c) $\phi_{\text{diff},1} = 120°$.

expected, the angular orientation of diffraction was 60° for the first TIR diffraction grating as depicted in Fig. 6(a), 90° for the second TIR diffraction grating as depicted in Fig. 6(b) and 120° for the third TIR diffraction grating as depicted Fig. 6(c). Also, the equal separations between bounces indicate that the polar angular orientation θ_{inc} of the beam incident onto the TIR grating is equal to that of the polar angular orientation $\theta_{\text{diff},1}$ of the diffracted beam.

We then experimentally measured the diffraction efficiencies, i.e., the power in the first diffraction order over that of the incident light, as a function of polar incidence angle for TIR diffraction gratings, both for TE and TM polarization. This was done by measuring the power of the diffracted light at the first bounce, and dividing it by the power of the incident light that arrives at an oblique angle from the coupling grating. In order to measure these powers of light, which normally would be trapped by total internal reflection inside the glass substrate, we attached a prism to the substrate with index matching liquid. The optical configuration with the attached prism was placed on the rotational stage, so as to allow variation of polar incidence angles with 1° steps.

Representative experimental and calculated results of diffraction efficiencies as a function of polar incidence angle for the first TIR diffraction grating with $\phi_{\text{diff},1} = 60°$ are presented in a Fig. 7. As evident, the measured diffraction efficiencies for TE polarization and for TM polarization are in a good agreement with the calculated results, as well as with those predicted in Fig. 4. Specifically, the predicted diffraction efficiency for the TIR diffraction grating with period $\Lambda = 0.3461\ \mu\text{m}$ and depth $d = 0.4100\ \mu\text{m}$ at the polar incidence angle $\theta_{\text{inc}} = 44°$ and azimuthal incidence angle $\phi_{\text{inc}} = 30°$ is about 97.2%, while the experimental value was about 91%. The slight difference can be attributed to TIR diffraction grating fabrication errors, which are not taken into account, as well as undesired absorption and light scattering in the photoresist layer. As with Bragg volume gratings, there is fast drop of diffraction efficiency for polar incidence angles ranging between 47° and 50°. For polar incidence angles beyond 50° the drop is due to the fact that total internal reflection no longer occurs and light escapes from the substrate.

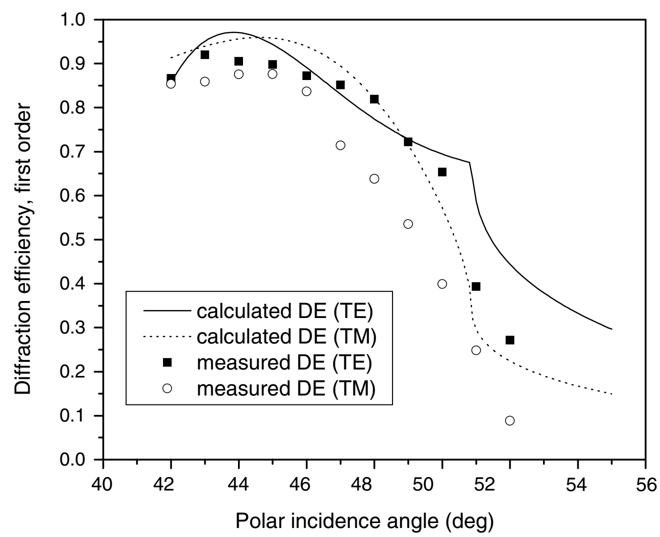

Fig. 7. Representative experimental and calculated diffraction efficiency as a function of polar incidence angle for a sinusoidal TIR diffraction grating. Grating period $\Lambda = 0.3461\ \mu\text{m}$, depth $d = 0.4100\ \mu\text{m}$, azimuthal incidence angle $\phi_{\text{inc}} = 30°$, and TE polarization.

5. Concluding remarks

We determined the main conditions and parameters for obtaining TIR diffraction gratings in conical mounting. These include the needed grating periods, azimuthal and polar incidence angles, and grating depths that also lead to high first order diffraction efficiency. The calculated and experimental results clearly demonstrate that it is indeed possible to control the angular orientation of light propagating inside the substrate, and achieve high diffraction efficiency from TIR diffraction gratings in conical mounting. We believe that with high diffraction efficiencies, such TIR diffraction gratings would be attractive in a variety of applications including display and interconnections.

References

[1] L.P. Boivin, Appl. Opt. 11 (1972) 1782.
[2] I. Gurwich, V. Weiss, L. Eisen, M. Meyklyar, A.A. Friesem, Proc. SPIE 5182 (2003) 212.

[3] A. Vasara, M.R. Taghizadeh, J. Turunen, J. Westerholm, E. Noponen, H. Ichikawa, J.M. Miller, T. Jaakkola, S. Kuisma, Appl. Opt. 31 (1992) 3320.
[4] J. Agostinelli, G. Harvey, T. Stone, H. Kobayashi, Appl. Opt. 18 (1979) 2500.
[5] S. Walker, J. Jahns, L. Li, W. Mansfield, D. Tennant, C. Roberts, L. West, N. Ailawadi, Appl. Opt. 32 (1993) 2494.
[6] E.G. Loewen, L.B. Mashev, E.K. Popov, Trans. SPIE 815 (1981) 66.
[7] E. Popov, L. Mashev, D. Maystre, Opt. Commun. 65 (1988) 97.
[8] J.R. Marciante, J.I. Hirsh, D.H. Raguin, E.T. Prince, J. Opt. Soc. Am. A 22 (2005) 299.
[9] M. Testorf, J. Jahns, J. Opt. Soc. Am. A 14 (1997) 1569.
[10] R. Shechter, Y. Amitay, A.A. Friesem, Appl. Opt. 41 (2002) 1236.
[11] R. Petit (Ed.), Electromagnetic Theory of Gratings, Springer-Verlag, Berlin, 1980.
[12] J.R. Marciante, D.H. Raguin, Opt. Lett. 29 (2004) 542.
[13] M.G. Moharam, T.K. Gaylord, J. Opt. Soc. Am. 73 (1983) 1105.